International Journal of General Medicine

Dovepress
Taylor & Francis Group

Open Access Full Text Article

REVIEW

Imaging Evaluation of Bone Tumors in the Cervical Spine: A Comprehensive Review

Man Sun, Xianghong Meng, MengShan Wu, Zhi Wang

Radiology Department, Tianjin Hospital, Tianjin, People's Republic of China

Correspondence: Zhi Wang, Email wangzhi13820256789@163.com

Abstract: The cervical spine, a critical junction between the head and torso, is a rare but significant site for both primary and metastatic tumors. While primary tumors of the cervical spine are uncommon, certain types, such as chordomas and giant cell tumors, are particularly notable for their potential to affect this region. Metastatic lesions, although more frequent, present unique diagnostic and therapeutic challenges due to the complex anatomy of the cervical spine. Imaging is indispensable for the evaluation of cervical spine tumors, serving as the foundation for diagnosis, treatment planning, and monitoring therapeutic outcomes. Radiography, CT and MRI are the primary modalities used to assess tumor morphology, extent and relationship to surrounding structures. However, imaging alone may not always yield a definitive diagnosis, as some tumors lack distinctive features. Nevertheless, a combination of clinical presentation, epidemiological factors, and imaging findings often enables radiologists and clinicians to narrow the differential diagnosis and guide further management. Precise imaging interpretation is essential to prevent devastating clinical consequences resulting from diagnostic error, such as irreversible neurological damage, avoidable death, and significant long-term disability. This review provides a comprehensive overview of tumors that can involve the cervical spine, emphasizing their clinical and imaging characteristics. By highlighting key diagnostic features and discussing the latest advancements in imaging technology, aims to enable physicians in radiology, pathology, and clinical departments to gain a more comprehensive understanding of the imaging, pathological, and clinical characteristics of cervical spine tumors, thereby reducing misdiagnosis rates and alleviating the burden on patients.

Keywords: cervical tumors, cervical spine, spine, X-ray, CT, MRI

Introduction

The cervical spine is situated between the skull and the relatively fixed thoracic spine, serving as a crucial bridge connecting the central nervous system to the trunk. Its complex structure, composed of seven vertebrae, intervertebral discs, facet joints, and numerous muscles and ligaments, provides a wide range of motion in three-dimensional space (such as flexion, extension, lateral bending, and rotation). This flexibility, however, also makes it biomechanically vulnerable and prone to injury. It supports the weight of the head and enables its multi-directional movement; the cervical spinal canal houses and protects the spinal cord, which is the essential pathway for all neural signals between the brain and the body; the transverse foramina provide a passage for the vertebral arteries, ensuring blood supply to the posterior part of the brain.[1–3] The upper cervical spine, in particular, has a highly complex anatomical structure.[4] The growth and compression of cervical tumors may affect vital tissues such as cranial nerves, the medulla oblongata, the cervical spinal cord, cervical nerve roots, and sympathetic nerves, significantly increasing the difficulty and risk of surgical treatment.[4] Additionally, the recurrence of benign tumors with unclear margins can mimic new or malignant disease, creating diagnostic ambiguity Cervical spine tumors are relatively rare, with limited clinical reports. Diagnosis requires a combination of imaging modalities, including X-rays, computed tomography (CT), magnetic resonance imaging (MRI), and pathological biopsies. Guided by the functional requirements of the spinal segments, the AO Spine classifications for the cervical spine define the upper cervical spine as encompassing three regions: (I) the occipital condyle and craniocervical articulation, (II) the C1 ring and C1–2 joint, and (III) the C2 vertebrae and C2–3 joint.[5] Imaging for upper cervical tumors may have limitations due to their unique location, necessitating comprehensive analysis of clinical manifestations. Although the incidence of cervical bone tumors is low, their diagnosis is complex and poses

Received: 30 August 2025
Accepted: 8 December 2025
Published: 25 December 2025

significant clinical challenges. Therefore, a review of the imaging diagnosis of this disease has important interdisciplinary significance. It provides a valuable template for rare disease thinking in clinical teaching; offers a clear differential diagnosis approach for radiology departments; helps the pathology department make more accurate judgments based on limited biopsy tissues in combination with imaging backgrounds; ultimately, it provides key evidence for treatment decisions and multi-disciplinary collaboration in oncology and spinal surgery, thereby systematically improving the level of diagnosis and treatment and benefiting patients.

Primary Cervical Spine Tumors

Primary cervical spine tumors originate from vertebral bodies or appendages, accounting for 10–15% of all spinal tumors. They are classified as benign, intermediate, or malignant.

Benign Primary Tumors

Osteoid Osteoma (OO)

Osteoid osteoma is a relatively rare type of benign bone tumor that often occurs within the cortex of the diaphysis of long tubular bones. It is most commonly observed in the femoral and tibial shafts, but its incidence in the spine is relatively low, accounting for approximately 7–12% of all spinal tumors.[6,7] In the cervical spine, it is relatively rare and mostly involves the appendages (include the vertebral arch, vertebral arch pedicle, lamina, transverse process, spinous process, and articular process). Osteoid osteoma is more prevalent in adolescents and young adults, with a peak incidence ranging from 10–20 years, there was a slight male predominance.[8] Osteoid osteomas are benign tumors composed of osteoblasts and the osteoid tissue they produce. It grows slowly and is characterized by nocturnal pain or exacerbation of pain at night. The pain is typically dull and may be accompanied by radiating pain.[8]

X-ray examination is less sensitive for detecting osteoid osteomas in the cervical spine and is prone to missed diagnoses. A typical osteoid osteoma may appear on plain radiographs as a small, isolated, round radiolucent defect with surrounding bone sclerosis.[7,8] CT (Figure 1E) has greater diagnostic value for osteoid osteoma because it can more clearly display the tumor nest, which is surrounded by reactive sclerotic bone. This is a typical manifestation of a cervical osteoid osteoma. MRI is sensitive in detecting the presence of a lesion, but it may not be as effective as CT in identifying the tumor nest. The lesion typically has low to moderate intensity on both T1 (Figure 1C) and T2 (Figure 1B and D).[7] Surrounding bone marrow edema and soft tissue inflammatory changes appear as high signal intensity on fat-suppressed T2WI (Figure 1A). The microscopic diagnosis of osteoid osteoma rests on identifying its central nidus: a focus of interconnecting osteoid trabeculae, lined with osteoblast cells, all embedded within a stroma of highly vascularized loose connective tissue that gives it a yellowish to reddish appearance (Figure 1F).

Clinically, nonsteroidal anti-inflammatory drugs (NSAIDs) can be used for conservative treatment. When the tumor is large and causes significant pain or spinal deformity, surgical resection should be considered. The recurrence rate after surgery depends on whether the tumor nest is completely removed. In recent years, with the continuous improvement in imaging techniques, CT-guided radiofrequency ablation (RFA)[9,10] has been shown to accurately locate the core area of the tumor (ie, the "tumor nest") and reduce the risk of unnecessary tissue damage while ensuring the effectiveness of treatment. Moreover, dynamic contrast-enhanced MRI (DCE-MRI) can be used to assess the tumor nest after radio-frequency ablation.

Aneurysmal Bone Cyst (ABC)

In 1942, Jaffe et al first described aneurysmal bone cysts (ABCs) of the spine, which are rare but aggressive benign tumors accounting for 1–2% of all primary bone tumors. The incidence of ABCs in the vertebral bodies represents 3–30% of all ABCs. Among vertebral lesions, the lumbar spine is most commonly involved, followed by the cervical and thoracic spine. Most ABCs involve the appendages, and one-third of ABCs do not involve the vertebral bodies.[11] Patients are usually younger than 20 years and often present with neck discomfort. ABCs of the axis vertebra can involve adjacent vertebrae or invade the spinal cord and neural structures. Fifty percent of patients with cervical spine ABCs have symptoms of spinal cord or nerve root compression.

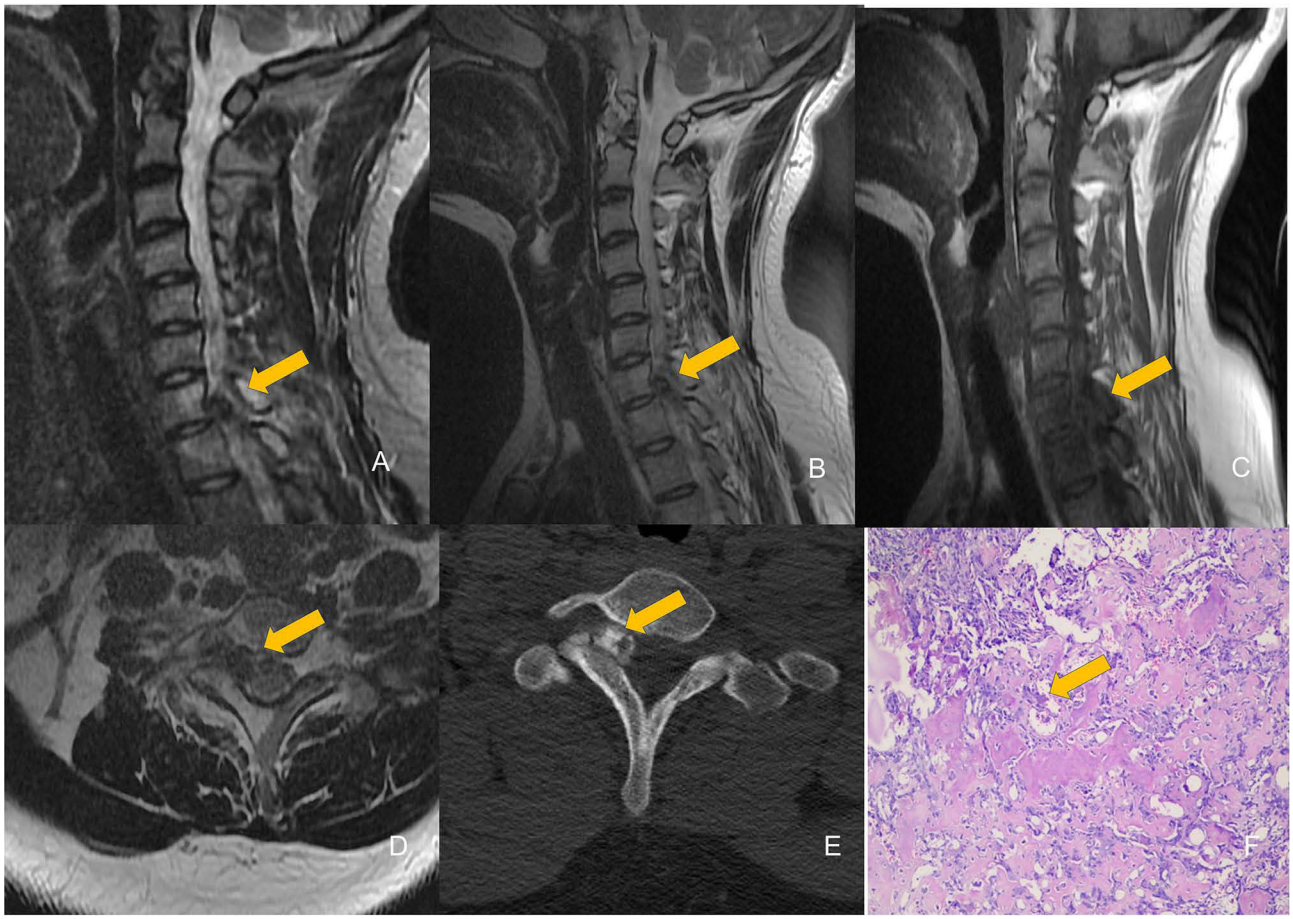

Figure 1 Osteoid osteoma of the Right Lamina of C7, Male, 18 years old, with right shoulder discomfort for over 1 year and worsening for over half a year. (**A**) Fat-suppressed T2WI sagittal view shows the lesion with low signal intensity, with extensive bone marrow edema visible around it. (**B** and **D**) T2WI sagittal and axial views show the lesion with low signal intensity. (**C**) T1WI sagittal view shows the lesion with low signal intensity. (**E**) CT plain scan reveals that the lesion is located in the right intervertebral foramen area, exhibiting heterogeneous and significant ossification, with no obvious invasion of the surrounding bone structures and no formation of a soft tissue mass. (**F**) HE (×20) shows that surfaces of the bone trabeculae are lined with osteoblasts and a small number of osteoclastic giant cells. Some of the osteoblasts (arrow) exhibit an epithelioid appearance with mild atypia.

On plain radiographs and CT scans, ABCs typically present as expansile, lytic bone destruction with a "soap bubble" appearance, characterized by thinning or discontinuity of the surrounding cortical bone. On MRI, the lesions show low signal intensity on T1WI and high signal intensity on T2WI. The internal signal is often heterogeneous, with visible septations that may be enhanced, whereas the intralesional components are not enhanced. The presence of multiloculated spaces and fluid–fluid levels are characteristic features.

Clinically, complete surgical resection is generally the treatment of choice. In cases where complete resection is not feasible due to the difficulty of achieving safe surgical removal in the involved area, selective arterial embolization is often employed.[11] Bisphosphonates, such as denosumab, are used to help control the growth of the lesion. Some studies have identified specific gene fusions, such as FGFR-USP6, in certain types of ABCs.[12] The detection of such molecular markers can aid in more accurate diagnoses and provide a basis for personalized treatment approaches.

Chondromyxoid Fibroma (CMF)

In 1948, Jaff first proposed and named[13] this condition, which is a rare benign primary bone tumor with local aggressiveness that accounts for 0.5% of all primary bone tumors. It predominantly occurs in the metaphyses of long tubular bones, especially around the knee joint. The spine is a rare site for CMF, with over 50 cases reported in the literature worldwide, representing 8% of all CMF cases and approximately 12 cases located in the cervical spine.[14] The

peak incidence age is between 10 and 20 years,[15,16] with no significant sex predilection. One-third of patients present with symptoms of neurological damage.

On CT scans, CMF appears as expansile, septated, cystic bone destruction with extensive cortical bone involvement.[15] Cortical breakthrough involving the soft tissue or spinal canal often indicates aggressive behavior. Compared with aneurysmal bone cysts and osteoblastomas, CMFs more frequently involve appendages, with rare calcification. On MRI,[16] the lesion shows intermediate or slightly low signal intensity on T1WI. On T2WI, the signal intensity varies from intermediate from low to high, depending on the content of fibrous, cartilaginous, and myxoid components within the lesion. On fat-suppressed T2WI, the lesion shows slightly high or high signal intensity. After contrast enhancement, the lesion demonstrated mild to moderate enhancement, with surrounding soft tissue edema but no soft tissue mass.

Clinically, en bloc resection is the preferred treatment. If en bloc resection is not feasible, curettage and bone grafting can be considered, the recurrence rate of this disease is highly expected with more than 25%.[17]

Benign Notochordal Cell Tumor (BNCT)

Benign Notochordal Cell Tumor (BNCT) was first documented by Darby[18] and originate from notochordal differentiation. Although the true incidence of BNCT remains unclear, it is most frequently encountered incidental findings in imaging studies performed for unrelated clinical indications.[19] For instance, the Yamaguchi study identified BNCTs in approximately 20% of cadaveric specimens;[19] however, the detection rate in clinical imaging is substantially lower, largely because many lesions are too small to be visualized. Nevertheless, an experienced radiologist may still be able to identify them.

BNCTs are most commonly reported in the sacrum and clivus, though they are also frequently observed in the cervical and lumbar spinal regions. Radiographically, these lesions are generally not detectable on plain films, CT or bone scans; larger BNCTs may exhibit sclerotic changes on CT while maintaining preserved cortical margins. MR imaging is considered the most sensitive modality for detecting BNCTs, typically showing a well-demarcated lesion with low to intermediate signal intensity on T1WI and high signal intensity on T2WI.[20,21] A characteristic radiological feature on contrast-enhanced MRI is the lack of significant enhancement. Moreover, no lesions have been reported to extend beyond the vertebral body into paraspinal or epidural spaces.[22] While MRI is highly valuable in suggesting the diagnosis of BNCT, histological examination remains essential for confirmation. Microscopically, BNCTs consist of sheets of vacuolated cells with eccentrically located nuclei. Characteristic physaliphorous cells, which contain multiple intracytoplasmic vacuoles, are interspersed throughout the lesion. Given their benign clinical behavior, BNCTs do not typically require surgical intervention. Instead, management generally involves careful and regular monitoring using CT and MRI.

Intermediate Primary Tumors

Giant Cell Tumors (GCTs)

Giant cell tumor of bone (GCTB) is a primary bone tumor that predominantly occurs in young adults aged 20–40 years, with a relatively high incidence in females.[23,24] It is most commonly found in peripheral bones such as the knee and radius. The sacrum is the most common site for GCTB in the axial skeleton.[23,24] In the spine, GCTB accounts for 2–3% of all spinal tumors, with a predilection for the cervical and sacral vertebrae.[25,26] Although it is defined as benign, 5–10% of GCTBs exhibit local aggressiveness and a tendency to recur. Rare cases of metastasis,[27] predominantly to the lungs, have also been reported. In the cervical spine, GCTB often invades the spinal canal and neural structures, causing pain, neurological dysfunction, or pathological fractures.

On plain radiographs, cervical GCTB typically presents as a “soap bubble” or purely lytic bone destruction. CT scans (Figure 2A, E and F) provide a clearer depiction of cortical thinning or bone invasion, often showing expansile lytic bone destruction with a well-defined sclerotic rim. The inner surface of the bony shell is often irregular, and the lesion margins are usually sharp without evidence of reactive bone sclerosis. In some cases, the tumor may exhibit a “moth-eaten” appearance with ill-defined margins, suggesting a greater risk of malignant transformation. In some instances, GCTB can breach the cortex to form extensive soft tissue masses. On MRI, the lesion appears as intermediate or low signal intensity on T1WI (Figure 2B) and mixed high signal intensity on T2WI (Figure 2C and G), T2-fs (Figure 2D), often presenting as intermediate or low signal intensity. Secondary aneurysmal bone cysts may also be observed. After contrast

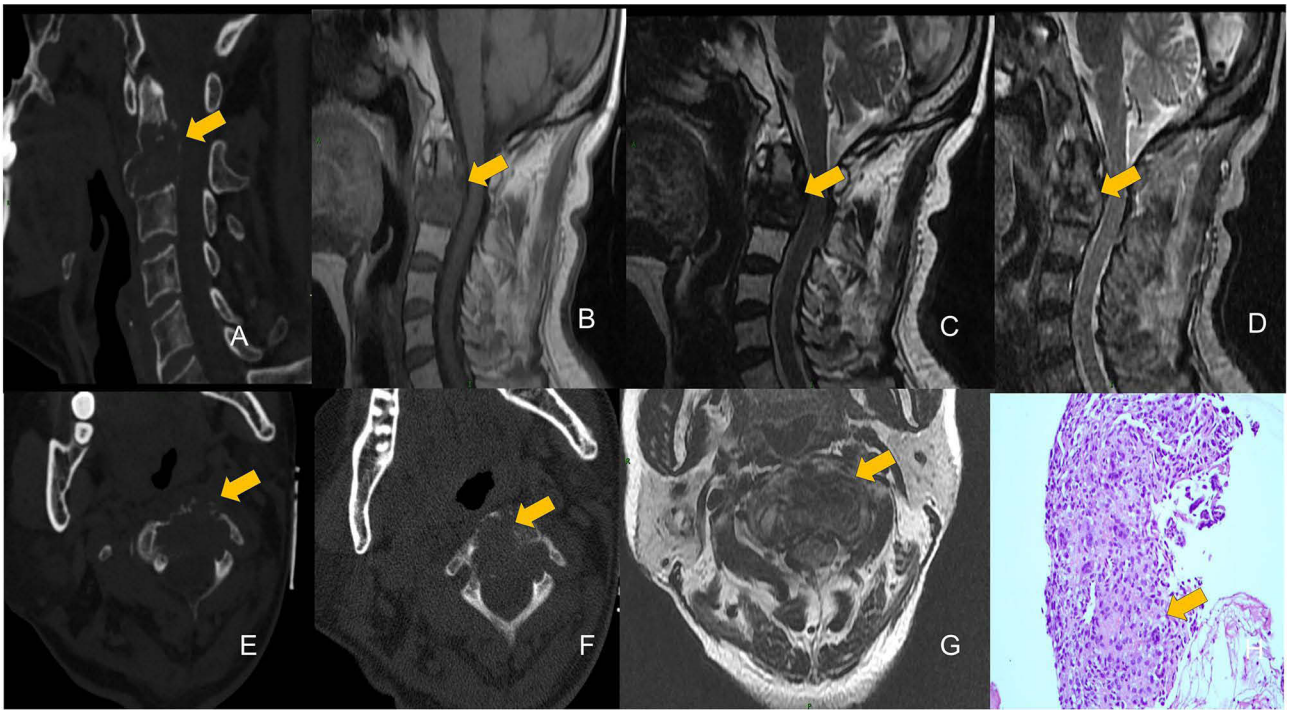

Figure 2 Giant Cell Tumor of the C2 Vertebral Body, Female, 64 years old, with neck and upper back pain for 3 months without obvious cause. (**A, E** and **F**) CT scan without contrast in sagittal and axial views shows expansile, lytic bone destruction of the axis vertebra. (**B**) T1WI shows the lesion with intermediate signal intensity. (**C** and **G**) T2WI in sagittal and axial views shows the lesion with intermediate and high signal intensity. (**D**) Fat-suppressed T2WI sagittal view shows the lesion with intermediate and high signal intensity. (**H**) HE (×20) shows that specimen shows small amounts of hyaline cartilage and large areas of coagulative necrosis. Scattered tumor tissue is occasionally observed amidst the necrotic areas, composed of short spindle-shaped cells, with occasional small, multinucleated giant cells (arrow).

enhancement, the tumor shows marked homogeneous or heterogeneous enhancement. 18F-FDG PET/CT effectively demonstrates the high metabolic activity and invasiveness of GCTB.[28] Under the microscope, GCTB presents a typical image characterized by a large number of multinucleated giant cells (Figure 2H) distributed unevenly throughout varying numbers of plump, round or spindle-shaped single-nucleated stromal cells.

Compared with peripheral bone lesions, cervical GCTB has a significantly poorer prognosis, with a recurrence rate as high as 80% after treatment. En bloc resection or curettage of the lesion is the optimal treatment approach. Adjuvant therapies, such as radiotherapy and anti-RANKL antibodies, can be used to reduce the risk of recurrence.[29,30] These findings suggest that GCTB is a highly vascular tumor and that preoperative embolization can reduce intraoperative bleeding and recurrence rates.

Malignant Primary Tumors

Chordoma

Chordoma is a rare malignant tumor originating from residual embryonic notochord cells and is commonly observed in middle-aged and elderly individuals over 40 years old, with lesions predominantly located at the ends of the spine.[31] It is a low-grade malignancy, and when it involves the spine, it most frequently affects the axis and sacrococcygeal vertebrae.[22–33] Chordomas arising from the axis often involve the clivus.

Radiologically, chordomas are characterized by their propensity to breach bone, dura mater, and neural tissues, with a tendency to infiltrate extradurally, intradurally, into the subarachnoid space, and around nerves.[34] On CT (Figure 3E–G), they typically present with lytic bone destruction, ill-defined margins, and occasional reactive bone sclerosis. Calcifications may be observed within some lesions. On MRI, owing to the high content of mucinous cells, the tumors appear as having intermediate to low signal intensity on T1WI (Figure 3C) and high signal intensity on T2-fs and T2WI (Figure 3A, B and D). They often have fibrous septations, resulting in heterogeneous signals and a "honeycomb" appearance. Soft tissue masses are usually present and tend to protrude anteriorly from the vertebral body. The spinal chordomas is composed of vacuolated cell cords

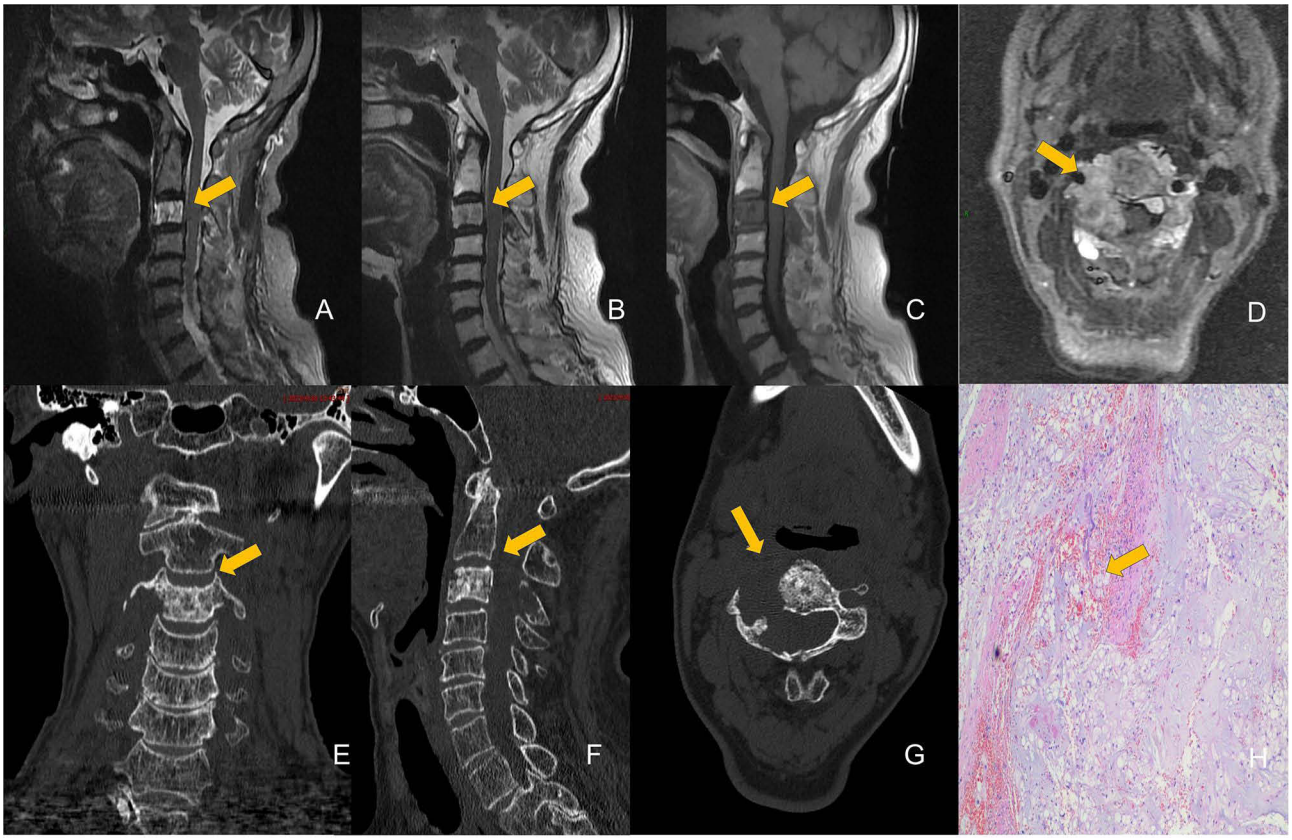

Figure 3 Chordoma of the C3 Vertebral Body, Female, 70 years old, with neck and shoulder pain for 1 week. (**A**) Fat-suppressed T2WI sagittal view shows the C3 vertebral body with intermediate and high signal intensity. (**B** and **D**) T2WI sagittal and axial views show the lesion with intermediate and high signal intensity. (**C**) T1WI sagittal view shows the lesion with intermediate signal intensity. (**E**–**G**) CT scan without contrast shows the lesion with expansile, lytic bone destruction, with sclerosis within the lesion. (**H**) HE (×10) shows that a large number of vacuolated cells (arrow) with hemorrhage.

under the microscope (Figure 3H), the size of the vacuoles varies with the larger ones reaching the full diameter of the cells, it is often accompanied by hemorrhage.

Surgical resection is the primary treatment for spinal chordomas.[29] When wide-margin resection is achievable, it significantly improves patient survival and local control rates. However, owing to the tendency of tumors to invade critical structures, the degree of surgical complexity is high, and the risk of complications is substantial. For lesions that cannot be completely resected, alternative surgical approaches, such as intralesional curettage combined with dissection surgery and stereotactic body radiotherapy (SBRT),[35] may be employed. Given the poor response of chordomas to conventional radiotherapy and chemotherapy, novel radiotherapeutic modalities such as proton beam therapy[36] are gaining attention as adjuvant postoperative treatments.

Synovial Sarcoma (SS)

Synovial sarcoma is a rare and aggressive malignant soft tissue tumor that is primarily composed of spindle cells and exhibits varying degrees of epithelial components. Despite its name, synovial sarcoma does not originate from synovial tissue. It is a mesenchymal tumor that may contain pleomorphic cells and scattered spindle cell components. This type of tumor predominantly occurs in the deep soft tissues of the extremities and accounts for more than 80% of all cases.[37] However, synovial sarcoma occurring within the spine is extremely rare, representing only approximately 5% of all synovial sarcomas.[38] Cervical spine synovial sarcoma has mostly been reported in case studies.[39] Cervical spine synovial sarcoma can occur at any age but is more common in young and middle-aged individuals, with a peak incidence between 15 and 40 years. There was a slight male predominance. Clinically, it may present as a painless or slowly enlarging mass, eventually leading to pain or neurological deficits.

CT (Figure 4E–G) typically reveals a round, oval, or lobulated soft tissue density mass with clear margins. On T1WI (Figure 4C), the lesion usually shows intermediate or slightly high signal intensity. On T2WI-fs and T2WI (Figure 4A, B and D), the signal intensity is heterogeneous, reflecting the varying composition of tumor tissue, fibrosis, necrosis, calcification, or hemorrhage within the lesion. The enhancement shows marked heterogeneous enhancement. The diagnosis of synovial sarcoma requires a combination of radiological examination, immunohistochemistry, and genetic testing. The presence of the SYT-SSX fusion gene is crucial for a definitive diagnosis.[40] Under the microscope, synovial sarcoma is composed of spindle-shaped cells arranged in bundles, interlacing patterns, or swirling patterns (Figure 4H).

The primary treatment for spinal synovial sarcoma is surgical resection, with an emphasis on achieving complete removal and ensuring negative margins.[41] Radiotherapy and chemotherapy are also employed to improve outcomes. The prognosis for patients with spinal synovial sarcoma remains poor.[42] Many patients present with distant metastases at the time of initial diagnosis, which contributes to a poor prognosis.[43]

Chondrosarcoma

Chondrosarcoma is the third most common primary malignant bone tumor, followed by osteosarcoma and Ewing's sarcoma. Solitary chondrosarcomas of the spine account for less than 10% of cases and most frequently occur in the thoracic spine, followed by the lumbar spine.[44,45] Currently, there are few reports of chondrosarcomas in the cervical spine both domestically and internationally. Forty percent of lesions originate in the appendages, with only 5% located in the vertebral bodies. Combined involvement of the vertebral bodies and appendages accounts for 45% of cases. Common symptoms include pain and palpable masses, with 50% of patients presenting with neurological symptoms. Chondrosarcomas can be graded into three levels: Grade 1, characterized by sparse cells and well-differentiated cells with an abundant hyaline cartilage matrix; Grade II, with a reduced hyaline cartilage matrix and increased cellular

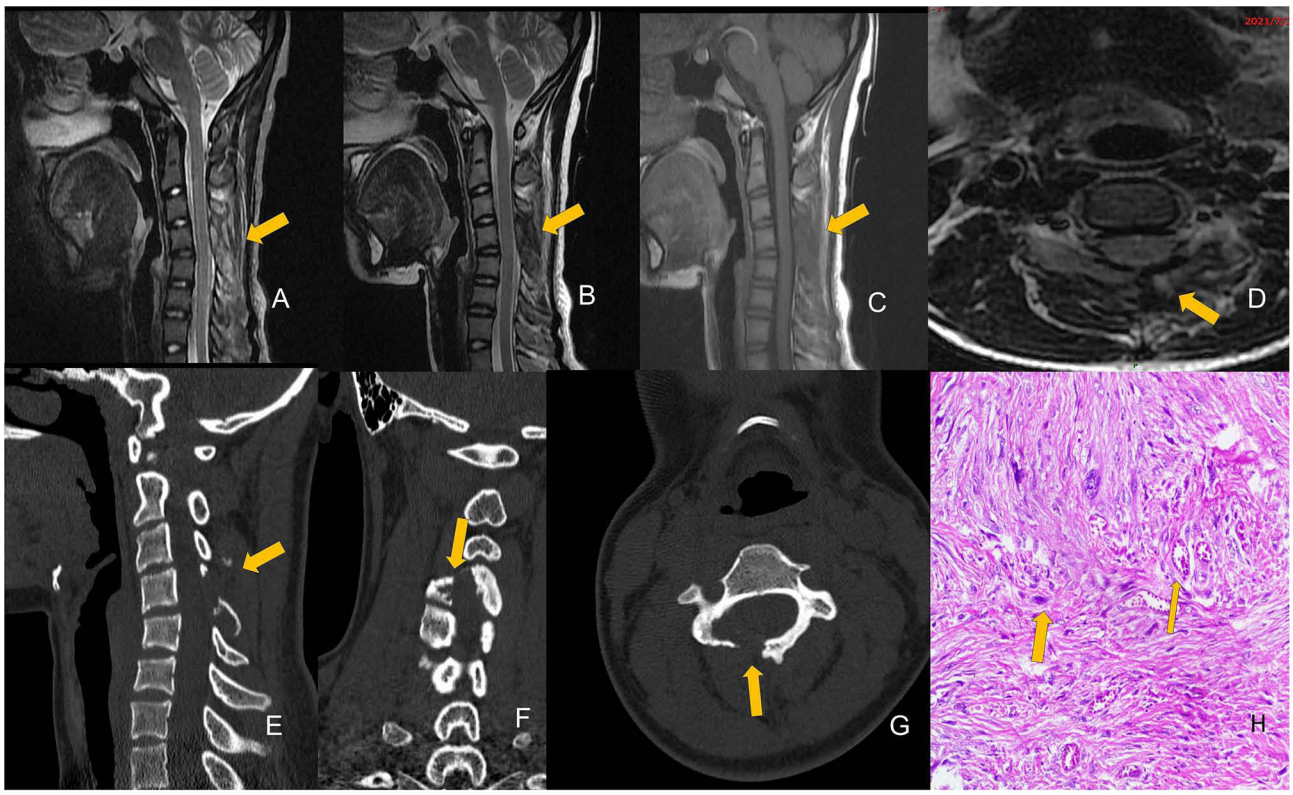

Figure 4 Synovial Sarcoma of the Right Lamina of C4, Female, 15 years old, with neck and shoulder pain accompanied by discomfort in the left upper arm for 2 months. (**A**) Fat-suppressed T2-weighted imaging (T2WI) sagittal view shows the right lamina of C4 with intermediate and slightly high signal intensity. (**B** and **D**) T2WI sagittal and axial views show the lesion with intermediate signal intensity. (**C**) T1-weighted imaging (T1WI) sagittal view shows the lesion with intermediate signal intensity. (**E**–**G**) CT scan without contrast shows the lesion with lytic bone destruction. (**H**) HE (×20) shows that tumor cells are spindle-shaped and amorphous (thick arrow), mostly exhibiting degenerative changes, with occasional tumor giant cells (thin arrow) and surrounding dense fibrous tissue hyperplasia.

https://doi.org/10.2147/IJGM.S564210

components; and Grade III, featuring densely packed cells with atypia. Seventy percent of patients with Grade III chondrosarcomas often have metastases.

On radiographs and CT scans, the lesions appear as irregular areas of bone destruction with lobulation and visible calcification of the cartilage matrix, which is better depicted on CT as punctate, linear, or semicircular changes. On MRI, the lesions show intermediate signal intensity on T1WI and high signal intensity on T2WI due to the presence of a hyaline cartilage matrix. Calcifications within the cartilage matrix appear as low signal intensity on all sequences. After contrast enhancement, low-grade chondrosarcomas show peripheral or septated enhancement, whereas high-grade chondrosarcomas exhibit nodular or diffuse enhancement. Under the microscope, chondrosarcoma can be observed in a background of cartilage-like or mucoid matrix. The tumor cells, which are of low to medium density, grow in nodular form and show mild to moderate atypia. Double-nucleated cells can be seen, and mitotic figures are rare or occasionally present.

Chondrosarcomas of the spine are not sensitive to radiotherapy or chemotherapy. Surgical resection is the most effective treatment, with a recurrence rate of 3–8%.[46] However, curettage or local resection results in a recurrence rate of up to 100%.[46]

Solitary Plasmacytoma (SP)

Solitary Plasmacytoma is also a common malignant spinal tumor that predominantly occurs in elderly individuals, with 70% of patients being over 50 years old. The thoracic and lumbar spine are the most frequently affected sites, followed by the cervical spine.[47,48] Some patients present with neck pain and limited mobility. Patients with Solitary plasmacytoma often have varying degrees of osteoporosis. Solitary plasmacytomas located in the upper cervical spine, owing to their greater position and lower load-bearing ability, rarely result in compression fractures of the affected vertebrae, thus presenting typical radiological features.

Radiographs are less sensitive for detecting lesions but often reveal bone destruction and pathological fractures (Figure 5A and B). On CT (Figure 5C–E), the lesions are characterized by lytic bone destruction with residual bone ridges and minimal osteoblastic activity. A typical appearance is the "pepper-pot" sign. On MRI, lesions usually show

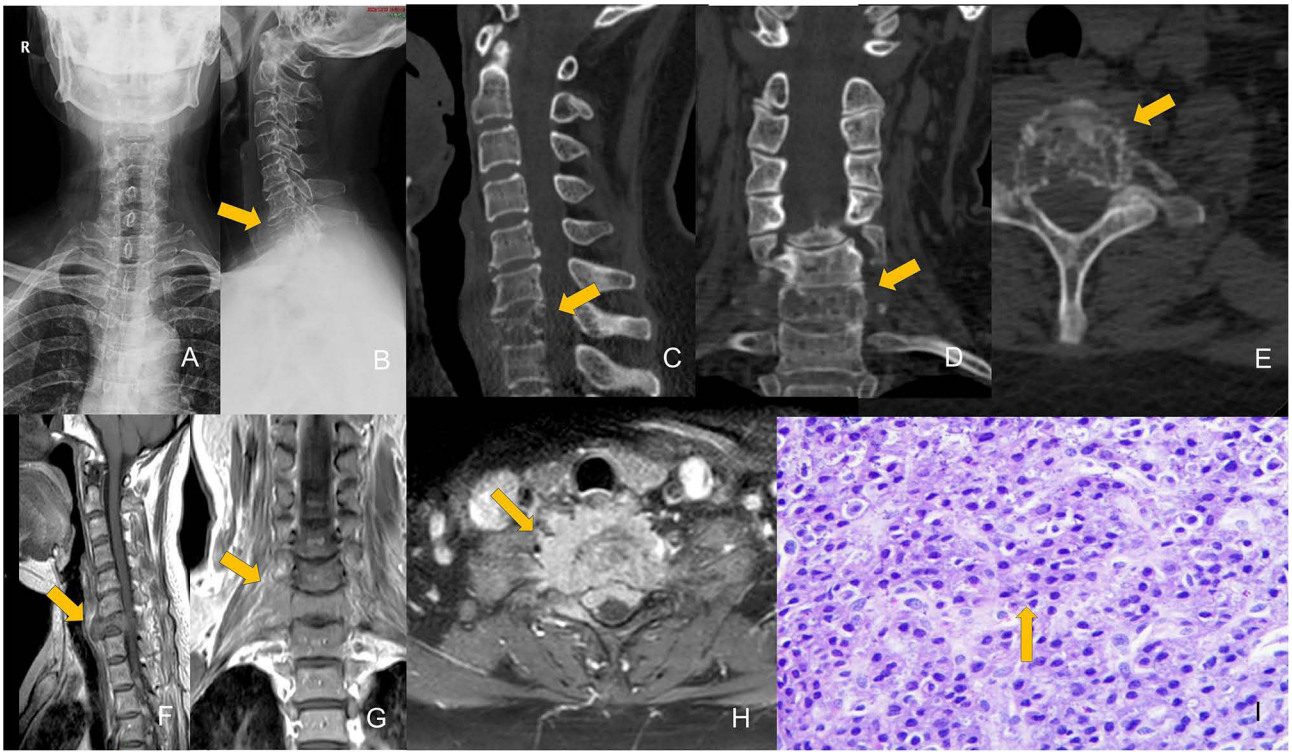

Figure 5 Solitary Plasmacytoma of the C7 Vertebral Body, Female, 55 years old, with right upper limb pain and numbness for half a year. (**A** and **B**) Radiographs show pathological fracture of the C7 vertebral body. (**C**–**E**) CT scan without contrast shows lytic bone destruction of the lesion with pathological fracture. (**F** and **G**) Contrast-enhanced T1WI in sagittal and coronal views shows moderate enhancement of the lesion. (**H**) Contrast-enhanced fat-suppressed T1WI axial view shows more pronounced enhancement of the lesion. (**I**) HE (×20) shows that multiple small round blue cells (arrow).

intermediate or low signal intensity on T1WI and intermediate or slightly high signal intensity on T2WI. On fat-suppressed T2WI, the signal is often slightly high. Owing to the dense nature of the plasma cells, cystic changes or necrosis are rare. Contrast enhancement typically results in homogeneous enhancement (Figure 5F–H), which is a distinguishing feature from metastatic tumors. Soft tissue masses are visible and often grow around the spinal canal. Histologically, solitary plasmacytoma are composed of sheets and clusters of plasma cells (Figure 5I). The neoplastic cells may demonstrate cytologic atypia, including enlarged size, irregular morphology, and occasionally prominent nuclei or nucleoli. Based on these features, they are designated by pathologists as atypical plasma cells.

The main treatment methods include surgical resection, radiotherapy, and chemotherapy. Studies[49,50] have shown that the combination of surgery and radiotherapy is effective and can effectively control local recurrence. For example, in one study,[50] 12 patients underwent en bloc vertebral resection via a combined anterior and posterior approach, with good postoperative outcomes51. Although solitary spinal plasmacytomas have a high local control rate, some patients may progress to multiple myeloma (MM). Therefore, regular follow-up is crucial to monitor disease progression and adjust the treatment plan in a timely manner.

Secondary Malignancies (Metastases)

Metastatic Tumor (MT)

Metastatic tumors are common malignant spinal tumors, accounting for approximately 5–10% of all spinal tumor. They predominantly occur in elderly individuals but are increasingly being diagnosed in younger individuals. They can be solitary or multiple. The most common site for spinal metastasis is the thoracic spine (50%-60%), followed by the lumbar spine (30%-35%), with the cervical spine being affected in approximately 10%-15% of cases.[51] The most common primary sites are the breast (21%), lung (19%), prostate (7.5%), kidney (7.5%), gastrointestinal tract (4.5%), and thyroid (2.5%).[52,53] However, some patients present without a known primary tumor, posing significant diagnostic challenges for radiologists. Some patients present with neck pain and limited mobility.

Spinal metastases can present as osteolytic, osteoblastic, or mixed lesions, each with distinct imaging characteristics. Osteolytic metastases CT (Figure 6E–G) typically appear as moth-eaten or geographic bone destruction with ill-defined

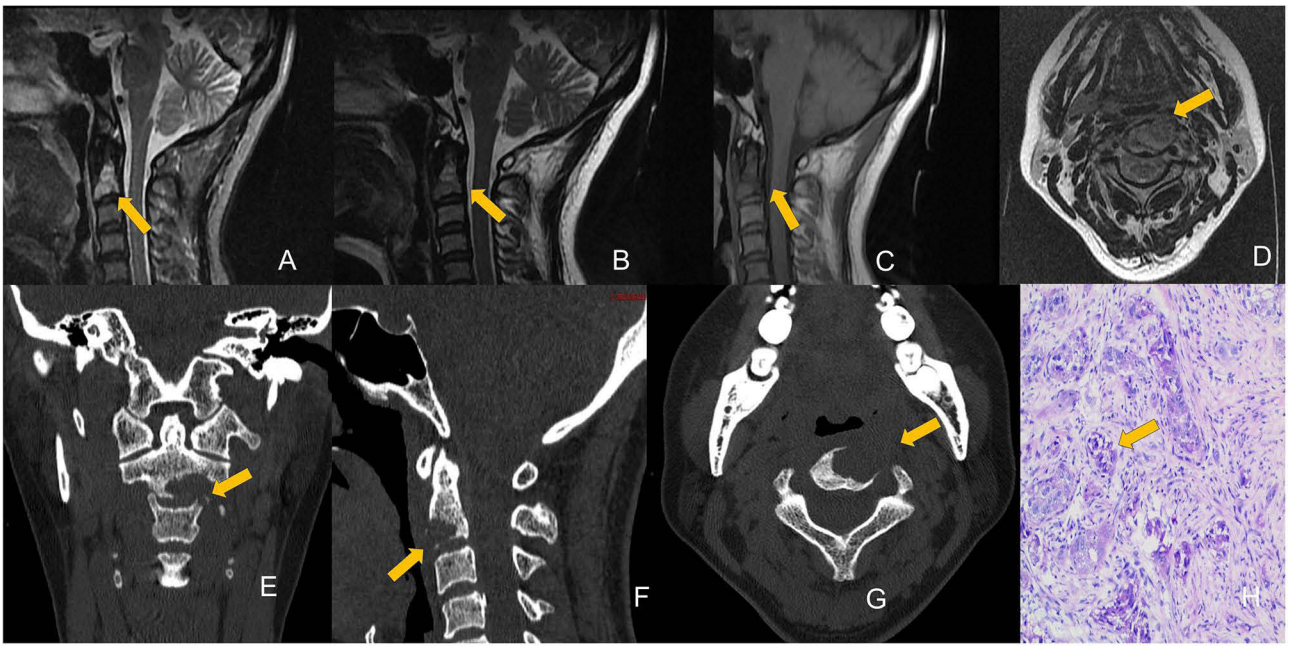

Figure 6 Squamous Cell Carcinoma Metastasis to the C2 Vertebral Body, Female, 45 years old, with neck pain and limited mobility for about 4 months. (**A**) Fat-suppressed T2WI sagittal view shows the axis vertebra with intermediate and slightly high signal intensity. (**B** and **D**) T2WI sagittal and axial views show the lesion with intermediate and slightly high signal intensity. (**C**) T1WI sagittal view shows the lesion with intermediate signal intensity. (**E–G**) CT scan without contrast shows the lesion with mild expansile, lytic bone destruction, no clear boundary. (**H**) HE (×20) shows that tumor tissue is observed to grow invasively within dense fibrous tissue. The tumor cells are arranged in clusters and nests (arrow), exhibiting large and hyperchromatic nuclei, eosinophilic cytoplasm, and visible nucleoli.

margins, which can be expansile. Calcifications are rarely observed on radiography or CT; On MRI, lesions usually show intermediate or low signal intensity on T1WI (Figure 6C) and intermediate or slightly high signal intensity on T2WI (Figure 6B and D). On fat-suppressed T2WI (Figure 6A), the signal is often slightly high. Hemorrhage, necrosis, and cystic changes are common,[54] resulting in heterogeneous density or signals within the lesion. Osteoblastic metastases demonstrate marked hyper-density with possible cortical thickening and irregular margins on radiography or CT (Figure 7E–G); On T1-weighted contrast-enhanced imaging, the lesion demonstrates heterogeneous and marked enhancement (Figure 7A–D) (contrast administration was not informative). Mixed metastases lesions has both osteolytic and osteoblastic destruction imaging features on CT or MRI. Soft tissue masses are frequently observed, often growing around areas of bone destruction. To improve the diagnostic accuracy for detecting spinal metastases, a learning algorithm based on CT images has been developed to automatically classify bone quality, aiding in the early detection of lesions.[55] Additionally, MRI and PET/CT have been used to evaluate lung cancer spinal metastases in mouse models, with PET/CT showing advantages in detecting microscopic metastases.[56] Under the microscope, the pathology of metastatic tumors varies depending on the primary tumor. In squamous cell carcinoma with bone metastasis (Figure 6H), the tumor cells exhibit features of squamous differentiation, including keratin pearl formation, intercellular bridges, and distinct cell junctions. The nuclei are large and display significant atypia. In contrast, bone metastasis from adenocarcinoma (Figure 7H) typically shows tumor cells arranged in nests, cords, or gland-like structures, similar to the morphology of the primary adenocarcinoma. However, these cells may exhibit varying degrees of atypia as a result of the metastatic process.

After the primary tumor is identified, metastatic tumors are generally treated with a combination of surgical resection, radiotherapy, and chemotherapy. Compared with traditional open surgery, for certain types of spinal metastases, such as those caused by non-small cell lung cancer, minimally invasive spinal surgery can reduce intraoperative blood loss and shorten the operative time, demonstrating better safety and efficacy. However, the risk of postoperative implant failure

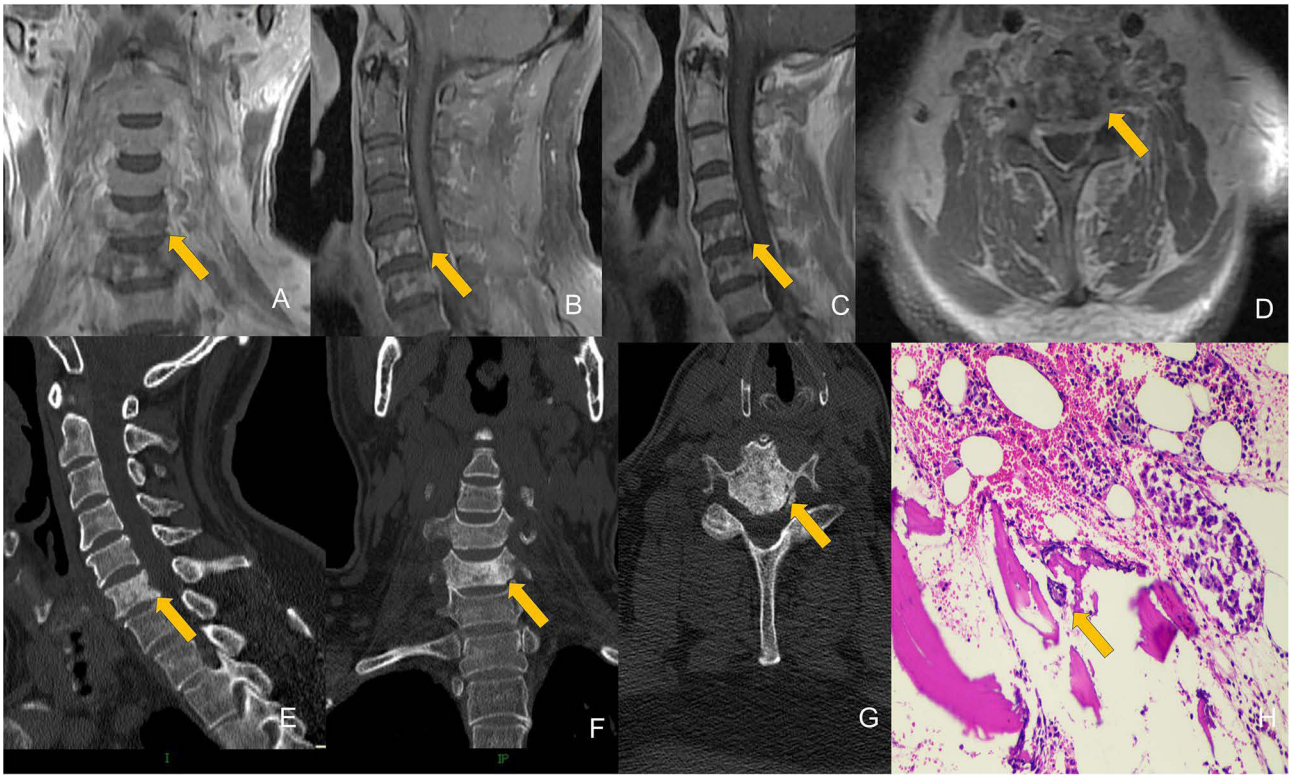

Figure 7 Adenocarcinoma Metastasis to the C5-C6 Vertebral Bodies, Male, 68 years old, with neck pain and limited mobility for about 12 months. (**A, C** and **D**) Contrast-enhanced T1WI in coronal, sagittal, and axial views shows heterogeneous and marked enhancement of the lesion. (**B**) Contrast-enhanced fat-suppressed T1WI sagittal view shows more pronounced enhancement of the lesion. (**E–G**) CT scan without contrast shows osteoblastic bone destruction of the C5-C6 vertebral bodies. (**H**) HE (×10) shows that scattered, mildly atypical cells (arrow) are present within the blood clot and between the bone trabeculae, without forming a distinct architectural pattern.

needs further study to identify relevant risk factors. Stereotactic body radiotherapy (SBRT) has been proven to effectively control local progression but also has limitations. On the other hand, the FLASH effect, a novel radiotherapy approach that achieves organ protection through ultrahigh-dose-rate irradiation, is gaining increasing attention but requires more biological research support. For example, in patients with prostate cancer spinal metastases, a multidisciplinary approach combining chemotherapy, radiotherapy, and surgery is becoming a trend.[57] In particular, with the advancement of medical imaging technology and genetic testing, the design of personalized treatment plans is becoming more feasible.

Conclusion

The severe, and often irreversible, consequences of diagnostic and therapeutic errors underscore the critical importance of accurate imaging evaluation. Misdiagnosing a cervical spine lesion—for instance, by confusing an aggressive primary tumor for a chordoma,[58] or failing to identify malignant transformation within a benign-appearing lesion—can directly lead to inappropriate management pathways. Such errors may result in delays in definitive treatment, the administration of futile therapies, or the selection of an incorrect surgical approach. Furthermore, the anatomical complexity and eloquence of the cervical spine mean that any inaccuracy in defining tumour extent or its relationship to critical structures —such as the vertebral arteries, spinal cord, or nerve roots—markedly elevates the risk of iatrogenic injury during surgical intervention. Potential complications include irreversible spinal cord injury and paralysis, cranial nerve deficits, vertebrobasilar stroke, and catastrophic hemorrhage. These adverse events directly contribute to increased perioperative mortality and profound long-term functional disability, which severely diminish the patient's quality of life and impose a substantial burden on healthcare systems.

Accurate preoperative diagnosis of cervical spine tumors is of paramount importance for selecting the appropriate clinical treatment strategy. Clinically, cervical spine tumors often present with nonspecific symptoms such as pain and limited mobility. However, patient age and radiological features can be characteristic. CT and MRI[59] are crucial for assessing the radiological features of tumors in the axis vertebrae and can help clinicians narrow diagnostic possibilities. To further increase diagnostic accuracy, radiologists are continuously exploring the potential of combining multiple imaging modalities. For example, studies have compared the performance of different imaging methods (such as CT and MRI) in detecting prostate cancer bone metastases and have found through meta-analysis that the combination of these modalities outperforms either method alone.[60] With technological advancements, in addition to traditional imaging techniques, functional imaging, such as perfusion imaging and diffusion-weighted imaging, has matured and has become a research focus in the field of cervical spine tumors.

In conclusion, as evidenced by the literature on diagnostic errors in cervical spine tumors a meticulous and systematic imaging approach (Table 1) is not merely an academic exercise but a fundamental clinical imperative for preventing patient harm and guiding therapies that preserve both life and function.

Table 1 Epidemiological and Imaging Features of Cervical Spine Tumors

		Age/Gender	CT Features	MRI Features	Key Signs
Primary benign tumor	Osteoid osteoma (OO)	10-20 years, Males > Females	Nidus with surrounding reactive sclerosis	T1WI low signal, T2WI medium or high signal, with significant surrounding bone marrow edema	Nidus, extensive bone marrow edema
	Aneurysmal bone cyst (ABC)	Mostly <20 years, no significant gender difference	Expansile, lytic bone destruction with thinning of cortical bone	T1WI low signal, T2WI high signal, no enhancement	Multiloculated, fluid-fluid levels
	Chondromyxoid fibroma (CMF)	10-20 years, no significant gender difference	Expansile, cystic bone destruction, possibly septated	T1WI iso- to slightly hypointense, T2WI heterogeneous signal, mild-to-moderate enhancement	Chondroid lobules, calcifications common
	Benign Notochordal Cell Tumor (BNCT)	Wide age range with no gender predilection	Sclerotic changes	T1WI low to intermediate signal intensity; T2WI high signal	Unifocal and small in size

(*Continued*)

Table 1 (Continued).

		Age/Gender	CT Features	MRI Features	Key Signs
Primary intermediate tumor	Giant cell tumor of bone (GCT)	20-40years (80%), Females > Males (2.5:1)	Eccentric, expansile, no sclerosis, no calcification	T1WI isosignal, T2WI heterogeneous high signal, moderate enhancement	Secondary aneurysmal bone cyst
Primary malignant bone tumor	Chordoma	30-60 years, Males > Females (2:1)	Central bone destruction, septations, calcifications, soft tissue mass	T1WI isosignal, T2WI high signal (brighter than intervertebral disc)	Mucinous-rich, high T2 signal, soft tissue mass protruding anteriorly
	Synovial sarcoma (SS)	15-40 years Males > Females	Lytic bone destruction, well-defined borders	T1WI iso- or slightly hyperintense, T2WI heterogeneous signal	Heterogeneous signal, frequent hemorrhage, cystic changes, necrosis
	Chondrosarcoma	30-70 years, Males > Females (2:1)	Irregular bone destruction, lobulated appearance, calcification within chondroid matrix	T1WI iso-signal, T2WI high signal, marked enhancement	Calcification within chondroid matrix in punctate, linear, or arcuate patterns
	Solitary plasmacytoma (SP)	Middle-aged to elderly, 70% > 50 years	Predominantly lytic destruction (osteoblastic rare), soft tissue mass	T1WI iso- to low signal, T2WI iso- to slightly high signal, moderate enhancement	Dense cellularity with homogeneous enhancement; soft tissue mass encircling the spinal canal
Secondary malignancy	Metastatic tumor (MT)	Middle-aged to elderly, history of primary malignancy	Bug-bite appearance of bone destruction, ill-defined borders, non-expansile without bone spicules	T1WI iso- to low signal, T2WI iso- to slightly high signal, mild enhancement	Heterogeneous signal, frequent hemorrhage, cystic changes, necrosis

Funding

This work was supported by the Tianjin Municipal Education Commission Scientific Research Plan Project, China (Grant No. 2023YXZX20).

Disclosure

The authors report no conflicts of interest in this work.

References

1. Ovsepyan AL, Smirnov AA, Pustozerov EA, et al. Biomechanical analysis of the cervical spine segment as a method for studying the functional and dynamic anatomy of the human neck. *Ann Anat*. 2022;240:151856. doi:10.1016/j.aanat.2021.151856
2. Coudert P, Lainé G, Pointillart V, et al. Tomodensitometric bone anatomy of the intervertebral foramen of the lower cervical spine: measurements and comparison of foraminal volume in healthy individuals and patients suffering from cervicobrachial neuralgia due to foraminal stenosis. *Surg Radiol Anat*. 2022;44(6):883–890. doi:10.1007/s00276-022-02941-8
3. Machino M, Yukawa Y, Imagama S, et al. Age-related and degenerative changes in the osseous anatomy, alignment, and range of motion of the cervical spine: a comparative study of radiographic data from 1016 patients with cervical spondylotic myelopathy and 1230 asymptomatic subjects. *Spine*. 2016;41(6):476–482. doi:10.1097/BRS.0000000000001237
4. Garg M, Sharma RK, Janu V, et al. C2 vertebra: an enigma for young spine/neurosurgeons. *J Neurol Surg B Skull Base*. 2024;86(1):92–97. doi:10.1055/a-2244-4761
5. Vaccaro AR, Lambrechts MJ, Karamian BA, et al. AO spine upper cervical injury classification system: a description and reliability study. *Spine J*. 2022;22(12):2042–2049. doi:10.1016/j.spinee.2022.08.005
6. Gokce E, Ayan E, Celikyay F, Acu B. Radiological imaging findings of a case with vertebral osteoid osteoma leading to brachial neuralgia. *J Clin Imaging Sci*. 2013;3:54. doi:10.4103/2156-7514.122324
7. Tah P, Alves C, Cardoso P, Ling T. A rare case of an osteoid osteoma of the cervical spine. *Case Reports Orthopedic Res*. 2020;3(2):79–87. doi:10.1159/000508371
8. Szathmari A, Almeida LCA, Beuriat PA, de Laurentis C, Vinchon M, Di Rocco F. Osteoid osteoma and osteoblastoma of the cervical spine in the pediatric population: analysis of the literature and experience with four operated cases. *Childs Nerv Syst*. 2024;41(1):69. doi:10.1007/s00381-024-06732-x
9. Singh DK, Katyan A, Kumar N, Nigam K, Jaiswal B, Misra RN. CT-guided radiofrequency ablation of osteoid osteoma: established concepts and new ideas. *Br J Radiol*. 2020;93(1114):20200266. doi:10.1259/bjr.20200266
10. Wang B, Han SB, Jiang L, et al. Percutaneous radiofrequency ablation for spinal osteoid osteoma and osteoblastoma. *Eur Spine J*. 2017;26(7):1884–1892. doi:10.1007/s00586-017-5080-0
11. Yun-yan MA. Imaging features and significance of preoperative embolization of spinal aneurysmal bone cyst in reducing intraoperative blood loss. *J Pract Radiol*. 2008;24(12):87–88+100.
12. Phan T, Tong J, Krivanek M, Graf N, Dexter M, Tumuluri K. Aneurysmal bone cyst of the orbit with USP6 gene rearrangement. *Ophthalmic Plast Reconstr Surg*. 2023;39(3):206–210. doi:10.1097/IOP.0000000000002287

13. Jaffe HL, Lichtenstein L. Chondromyxoid fibroma of bone: a distinctive benign tumor likely to be mistaken especially for chondrosarcoma. *Arch Pathol*. 1948;45:541–551.
14. Subach BR, Copay AG, Martin MM, Schuler TC, Romero-Gutierrez M. An unusual occurrence of chondromyxoid fibroma with secondary aneurysmal bone cyst in the cervical spine. *Spine J*. 2010;10(2):e5–e9. doi:10.1016/j.spinee.2009.11.016
15. Taghipour Zahir S, Sefidrokh Sharahjin N, Sadlu Parizi F, Rahmani K. Chondromyxoid fibroma of two cervical vertebrae with involvement of surrounding soft tissue: radiologic diagnostic dilemma. *Iran J Radiol*. 2015;12(4):e19273. doi:10.5812/iranjradiol.19273
16. Li C, Li S, Hu W. Chondromyxoid fibroma of the cervical spine: a case report. *World J Clin Cases*. 2022;10(17):5748–5755. doi:10.12998/wjcc.v10.i17.5748
17. Dürr HR, Lienemann A, Nerlich A, Stumpenhausen B, Refior HJ. Chondromyxoid fibroma of bone. *Arch Orthop Trauma Surg*. 2000;120(1–2):42–47. doi:10.1007/pl00021214
18. Darby AJ, Cassar-Pullicino VN, McCall IW, Jaffray DC. Vertebral intra-osseous chordoma or giant notochordal rest? *Skeletal Radiol*. 1999;28(6):342–346. doi:10.1007/s002560050528
19. Yamaguchi T, Suzuki S, Ishiiwa H, Shimizu K, Ueda Y. Benign notochordal cell tumors: a comparative histological study of benign notochordal cell tumors, classic chordomas, and notochordal vestiges of fetal intervertebral discs. *Am J Surg Pathol*. 2004;28(6):756–761. doi:10.1097/01.pas.0000126058.18669.5d
20. Grabovska D, Strumfa I, Ositis J, Liepniece-Karele I, Balodis A. Benign notochordal cell tumours: case report and literature review. *Diagnostics*. 2024;14(13):1330. doi:10.3390/diagnostics14131330
21. Ulusoy OL, Tutar S, Ozturk E, Mutlu A. Benign notochordal cell tumor of C2 vertebra mimicking metastasis. *Spine J*. 2016;16(6):e383. doi:10.1016/j.spinee.2015.12.015
22. Iorgulescu JB, Laufer I, Hameed M, et al. Benign notochordal cell tumors of the spine: natural history of 8 patients with histologically confirmed lesions. *Neurosurgery*. 2013;73(3):411–416. doi:10.1227/01.neu.0000431476.94783.c6
23. Parmeggiani A, Miceli M, Errani C, Facchini G. State of the art and new concepts in giant cell tumor of bone: imaging features and tumor characteristics. *Cancers*. 2021;13(24):6298. doi:10.3390/cancers13246298
24. Dahlin DC, Cupps RE, Johnson EW. Giant-cell tumor: a study of 195 cases. *Cancer*. 1970;25(5):1061–1070. doi:10.1002/1097-
25. Shirakuni T, Tamaki N, Matsumoto S, Fujiwara M. Giant cell tumor in cervical spine. *Surg Neurol*. 1985;23(2):148–152. doi:10.1016/0090-3019(85)90333-7
26. Müther M, Schwake M, Suero Molina E, et al. Multiprofessional management of giant cell tumors in the cervical spine: a systematic review. *World Neurosurg*. 2021;151:53–60. doi:10.1016/j.wneu.2021.04.006
27. Viswanathan S, Jambhekar NA. Metastatic giant cell tumor of bone: are there associated factors and best treatment modalities? *Clin Orthop Relat Res*. 2010;468(3):827–833. doi:10.1007/s11999-009-0966-8
28. Dejust S, Jallerat P, Soibinet-Oudot P, Jouannaud C, Morland D. Multimodality imaging features of a misleading sacral giant cell tumor in 18F-FDG PET/CT, bone scan, and MRI. *Clin Nucl Med*. 2020;45(10):800–801. doi:10.1097/RLU.0000000000003148
29. Chakravarti A, Spiro IJ, Hug EB, Mankin HJ, Efird JT, Suit HD. Megavoltage radiation therapy for axial and inoperable giant-cell tumor of bone. *J Bone Joint Surg Am*. 1999;81(11):1566–1573. doi:10.2106/00004623-199911000-00008
30. Yokogawa N, Murakami H, Demura S, et al. Total spondylectomy for Enneking stage III giant cell tumor of the mobile spine. *Eur Spine J*. 2018;27(12):3084–3091. doi:10.1007/s00586-018-5761-3
31. Hong S, Shinya Y, Lakomkin N, et al. Predicting the need for occipitocervical fusion for patients with lower clival chordoma: a single-center retrospective study. *World Neurosurg*. 2024;187:e321–e330. doi:10.1016/j.wneu.2024.04.081
32. Pena-Burgos EM, Torena Lerchundi N, Fuentes-Sánchez J, Tapia-Viñe M, Fernández-Baíllo N, Pozo-Kreilinger JJ. Notochordal cell derived lesions: a 55-year casuistic analysis of 50 cases with radiologic-pathologic correlation in a tertiary referral hospital, and literature review. *Eur Spine J*. 2024;33(9):3315–3323. doi:10.1007/s00586-024-08419-y
33. Hyun SJ, Rhim SC, Riew KD. A combined posterior, lateral, and anterior approach to ventrolaterally situated chordoma of the upper cervical spine. *Surg Neurol*. 2009;72(4):409–413. doi:10.1016/j.surneu.2008.11.017
34. Santín-Amo JM, Puñal-Rodríguez JA, Frieiro-Dantas C, Serramito-García R, Beiras-Sarasquete C. Cordoma sacrococcígeo [Sacrococcygeal chordoma]. *Rev Neurol*. 2013;57(10):471–472. doi:10.33588/rn.5710.2013267
35. Lockney DT, Shub T, Hopkins B, et al. Spinal stereotactic body radiotherapy following intralesional curettage with separation surgery for initial or salvage chordoma treatment. *Neurosurg Focus*. 2017;42(1):E4. doi:10.3171/2016.9.FOCUS16373
36. Miladinovic V, Klaver YLB, Krol ADG, et al. Robust IMPT and follow-up toxicity in skull base chordoma and chondrosarcoma-a single-institution clinical experience. *Strahlenther Onkol*. 2024;200(12):1066–1073. doi:10.1007/s00066-024-02280-0
37. Sakellaridis N, Mahera H, Pomonis S. Hemangiopericytoma-like synovial sarcoma of the lumbar spine. *Case Report J Neurosurg Spine*. 2006;4(2):179–182. doi:10.3171/spi.2006.4.2.179
38. Kim J, Lee SH, Choi YL, Bae GE, Kim ES, Eoh W. Synovial sarcoma of the spine: a case involving paraspinal muscle with extensive calcification and the surgical consideration in treatment. *Eur Spine J*. 2014;23(1):27–31. doi:10.1007/s00586-013-3034-8
39. Shah WU, Shujaat SD, Ullah N, Mansoor S. Synovial sarcoma of cervicodorsal spine: a case report. *J Pak Med Assoc*. 2018;68(7):1100–1104.
40. Cao Y, Jiang C, Chen Z, Jiang X. A rare synovial sarcoma of the spine in the thoracic vertebral body. *Eur Spine J*. 2014;23 Suppl 2(S2):228–235. doi:10.1007/s00586-013-3099-4
41. Blackmon S. Synovial Sarcoma. *Atlas Neoplastic Pulmonary Dis*. 2010;51.
42. Najib S, Saleem T, Nadhim A, Sen S. A rare case of monophasic synovial sarcoma of thoracic vertebra. *Case Rep Med*. 2018;2018:2313927. doi:10.1155/2018/2313927
43. Demir MK, Fakir E, Furuncuoglu Y, Alıcı S, Argon A, Koca S. Synovial sarcoma with multiple vertebrae metastases causing multilevel thoracic spinal cord compressions. *Spine J*. 2016;16(6):e363–e364. doi:10.1016/j.spinee.2015.11.063
44. Katonis P, Alpantaki K, Michail K, et al. Spinal chondrosarcoma: a review. *Sarcoma*. 2011;2011:378957. doi:10.1155/2011/378957
45. Riedel RF, Larrier N, Dodd L, Kirsch D, Martinez S, Brigman BE. The clinical management of chondrosarcoma. *Curr Treat Options Oncol*. 2009;10(1–2):94–106. doi:10.1007/s11864-009-0088-2
46. Boriani S, De Iure F, Bandiera S, et al. Chondrosarcoma of the mobile spine: report on 22 cases. *Spine*. 2000;25(7):804–812. doi:10.1097/00007632-200004010-00008

47. Pashayan R, Cavanaugh WM, Warshel CD, Payne DR. Plasmacytoma of the cervical spine: a case study. *J Chiropr Med*. 2017;16(2):170–174. doi:10.1016/j.jcm.2015.10.001
48. Lang N, Su MY, Yu HJ, Lin M, Hamamura MJ, Yuan H. Differentiation of myeloma and metastatic cancer in the spine using dynamic contrast-enhanced MRI. *Magn Reson Imaging*. 2013;31(8):1285–1291. doi:10.1016/j.mri.2012.10.006
49. Charalampous C, Claveau JS, Kapoor P, et al. Solitary plasmacytoma: single-institution experience, and systematic review and meta-analysis of clinical outcomes. *Blood Adv*. 2025;9(7):1559–1570. doi:10.1182/bloodadvances.2024013355
50. Wu M, Cai L, Yan F, et al. Zhongguo Xiu Fu Chong Jian Wai Ke Za Zhi. *Zhongguo xiu fu chong jian wai ke za*. 2018;32(2):195–202. doi:10.7507/1002-1892.201709107
51. Truong VT, Al-Shakfa F, Phan P, et al. Does the region of the spine involved with metastatic tumor affect outcomes of surgical treatments? *World Neurosurg*. 2021;156:e139–e151. doi:10.1016/j.wneu.2021.09.014
52. Kim K, Ha M, Kim SJ. Comparative study of different imaging modalities for diagnosis of bone metastases of prostate cancer: a bayesian network meta-analysis. *Clin Nucl Med*. 2024;49(4):312–318. doi:10.1097/RLU.0000000000005078
53. Bilsky MH, Shannon FJ, Sheppard S, Prabhu V, Boland PJ. Diagnosis and management of a metastatic tumor in the atlantoaxial spine. *Spine*. 2002;27(10):1062–1069. doi:10.1097/00007632-200205150-00011
54. Baker JF, Shafqat A, Devitt A, McCabe JP. Stabilization of metastatic lesions affecting the second cervical vertebra. *J Craniovertebr Junction Spine*. 2015;6(2):56–59. doi:10.4103/0974-8237.156041
55. Rajkumar SV. Multiple myeloma: 2018 update on diagnosis, risk-stratification, and management. *Am J Hematol*. 2018;93(8):981–1114. doi:10.1002/ajh.25117
56. Peng S. Learning-based bone quality classification method for spinal metastasis. arXiv preprint arXiv:2402.08910. 2024. doi:10.1007/978-3-030-32692-0_49
57. Laufer I, Rubin DG, Lis E, et al. The NOMS framework: approach to the treatment of spinal metastatic tumors. *Oncologist*. 2013;18(6):744–751. doi:10.1634/theoncologist.2012-0293
58. Zhou H, Yang X, Wang R, Liu X, Liu Z, Wei F. Misdiagnosis of primary dumbbell chordoma of the cervical spine. *Asia Pac J Clin Oncol*. 2024;20(5):620–626. doi:10.1111/ajco.13968
59. Rothwell J, Jha S. Spinal epidural abscess and medical malpractice: the role of diagnostic imaging in legal cases. *Acad Radiol*. 2025;32(Supplement 1):S144–S148. doi:10.1016/j.acra.2025.04.027
60. Hu W, Liu Z, Xiao X, Yang Y, Sun Z, Wang X. Comparison of diagnostic efficacy of MRI and PET/CT in lung cancer of mouse with spinal metastasis. *Cell Mol Biol*. 2020;66(3):138–142. doi:10.14715/cmb/2020.66.3.21